Geofísica Internacional (2007), Vol. 46, Num. 3, pp. 199-209

Tidal currents in the Yucatan Channel

Fátima Carrillo González[1], José Ochoa[2,3,*], Julio Candela[2], Antonio Badan[2], Julio Sheinbaum[2] and Juan Ignacio González Navarro[2]

[1] *Centro Universitario de la Costa, Universidad de Guadalajara, Guadalajara, Mexico*

[2] *Departamento de Oceanografía Física, Centro de Investigación Científica y de Educación Superior de Ensenada, Ensenada, Baja California, Mexico*

Received: February 16, 2007; accepted: June 20, 2007

Resumen

Se presentan, a detalle sin precedente, las características de las corrientes de marea O_1, K_1, M_2 y S_2 en el canal de Yucatán. Mapas de los parámetros que definen las elipses, como son las amplitudes en los ejes principales, la orientación, la fase y la razón-señal-ruido se obtienen, por el clásico análisis armónico en mediciones de 10 meses en duración, en 197 puntos que cubren ampliamente un plano vertical del canal. En acuerdo con reportes anteriores, las señales diurnas O_1 y K_1 dominan, demostrándose aquí que sus amplitudes alcanzan, en la parte profunda y Este, 17 y 19 $cm{\cdot}s^{-1}$. El análisis también revela señales semidiurnas M_2 y S_2 muy débiles con amplitudes máximas de 2 y 1$cm{\cdot}s^{-1}$. Las elipses son muy alargadas (*i.e.* con excentricidad cercana a uno) y orientadas al nornoroeste. Los valores de la razón señal a ruido indican que los parámetros de las dos constituyentes diurnas se encuentran bien determinados, mientras que las semidiurnas quedan muy contaminadas por el ruido. El rasgo más sobresaliente y novedoso de las observaciones es la intensificación de las componentes diurnas en el lado Este y profundo del Canal. Las amplitudes del transporte a través del Canal debidas a O_1, K_1, M_2 y S_2 son 11.7, 12.5, 1.2 y 1.0 *Sv*, todas bien determinadas por encima del ruido.

Palabras clave: Corrientes, mareas, Yucatán.

Abstract

Currents data from a ten-month period at 197 measuring points covering all Yucatan Channel were processed by harmonic analysis to estimate tidal parameters for the O_1, K_1, M_2 and S_2 components. The highly detailed coverage confirms the known dominance for the O_1 and K_1 diurnal components, but also showed, for the first time, their intensification in the deep eastern margin of the channel where maximum amplitudes in main axis are 17 and 19 $cm{\cdot}s^{-1}$. The data also confirms weak semi-diurnal components, of which the most intense, M_2 and S_2, have amplitudes only up to 2 $cm{\cdot}s^{-1}$. The tidal ellipses were elongated (*i.e.* with eccentricities close to one) in the NNW direction. The O_1, K_1, M_2 and S_2 contributions in transport variability through the channel have amplitudes of 11.7, 12.5, 1.2 and 1.0 *Sv*, all well determined above noise.

Key words: Currents, tides, Yucatán.

Introduction

This study presents detailed distributions of amplitudes, orientations and phases for the O_1, K_1, M_2 and S_2 components of tides in the complete Yucatan Channel vertical section. Details on the field work may be found in a Master Thesis by Carrillo (2001). This data set is a part of the CANEK Project, which was mainly intended to provide a direct determination of transport through the Yucatan Channel. We used harmonic analysis of the current flow time series which confirm the previously known character of the diurnal tides, but a new significant finding is the observation of intense tidal currents in the deep eastern margin of the section, where tides can contribute up to 80% of the current variance. The dynamical origin of this intensification and of the corresponding mean return flow towards the Caribbean (Sheinbaum *et al*., 2002, Ochoa *et al*., 2001), are unknown.

Below a depth of 1000 m the isobaths of the channel between the Caribbean Sea and the Gulf of Mexico turns from NNE in the Caribbean to NNW in the Gulf. At the ocean surface, the channel is 200 km wide between Cabo Catoche, Mexico and Cabo San Antonio, Cuba (Hansen and Molinari, 1979, Badan *et al*., 2005, Carrillo, 2001). The depth of the sill is 2040 m (Figures 1 and 2). The flow in the Yucatan Channel is an essential component of the regional circulation, which feeds the Gulf Stream. It influences the dynamics and circulation of the Gulf of Mexico and of the North Atlantic.

Earlier studies show that tidal amplitudes off the Yucatan Peninsula as well as off eastern Cuba are small (Kjerfve 1981, Carrillo 2001). Sea level tidal ranges, even for the semi-diurnal components which are the largest, do not exceed 10 *cm* in amplitude. They have been called microtidal regimes (Kjerfve, 1981). However,

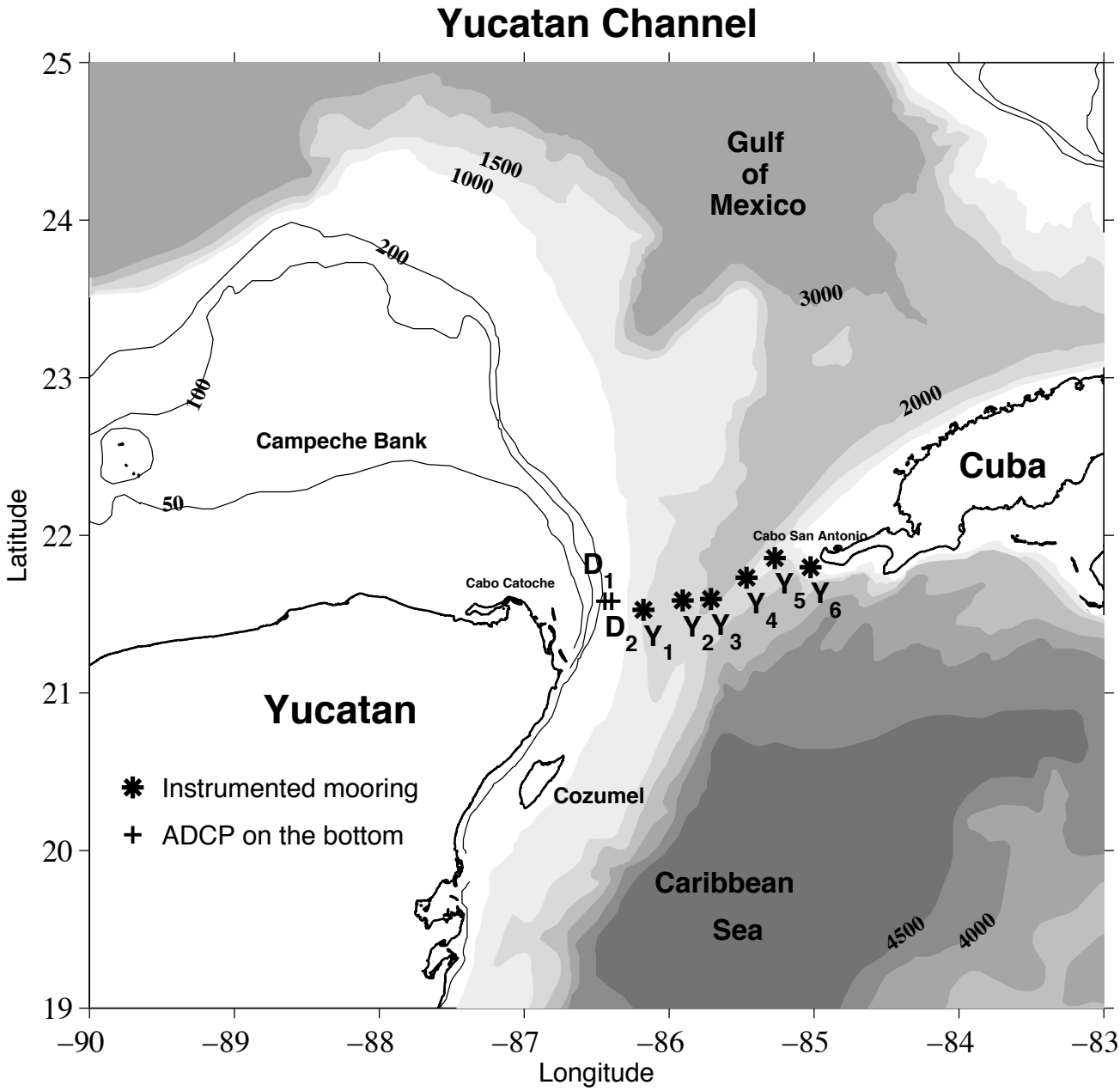

Fig. 1. Mooring (asterisks and plus signs) positioning in the Yucatan Channel, named from West to East D_1, D_2, Y_1, Y_2, Y_3, Y_4, Y_5 and Y_6 (D_1 and D_2 are at the plus signs, very close together in the western limit of the mooring array).

small sea level amplitudes do not necessarily imply that the associated currents must be weak. In this case, the currents are indeed small in most of the channel, as shown by direct measurements in the area (Hansen and Molinari, 1979, Maul *et al*., 1985) and by measurements in this study. Hansen and Molinari (1979) carried out a one-month moored current measurement near the bottom and found that the dominant tidal ellipses are diurnal, almost rectilinear, and oriented parallel to the isobaths. Their Figure 2 shows that the dominant oscillations are diurnal and assuming superposition of O_1 and K_1 they should have amplitudes of approximately 4 $cm{\cdot}s^{-1}$. Maul *et al*. (1985, their Table 4) provide information from a nine-month record of current measurements near the center of the channel, at a point 15 km west of the sill and 145 m above the bottom. They estimate tidal amplitudes of 3.8/0.6 $cm{\cdot}s^{-1}$ for the O_1 major/minor axis, and 3.0/0.8 for K_1.

These currents are weak, but the corresponding transport (i. e. full amount of water crossing the channel) oscillations

are large. The channel cross-section area is close to 200 km^2; thus a uniform velocity of 1 $cm{\cdot}s^{-1}$ implies a transport of 2 *Sv* (1 *Sverdrup*=10^6 $m^3{\cdot}s^{-1}$). Hansen and Molinari (1979) and Maul *et al*. (1985) estimate amplitudes of tidal transport of 8 *Sv* for the O_1 and K_1 diurnal components. In the case of semi-permanent transport estimates, due to slowly varying geostrophic currents, even a weak tidal signal can introduce a significant contamination. Ochoa *et al*. (2001) argue that the main source of uncertainty in their own geostrophic transport estimates came from tidal currents. The areal coverage provided by the measurements used in this study includes the full channel vertical section, which is the most complete data set to date. Earlier measurements were extremely poor in spatial coverage.

In the following section the data used in this study are described. The third section describes the analysis, results and discussions, including the maps of ellipse components. The final section reports our conclusions.

Data

Direct current measurements were obtained for a 10-month period (August 1999 to June 2000), with a 1-hour sampling interval. The instruments were distributed in eight moorings, designated by D_1, D_2, Y_1, Y_2, Y_3, Y_4, Y_5 and Y_6, and positioned between the Yucatan Peninsula and Cuba (Figure 1). The upper end of each mooring was instrumented with an Acoustic Doppler Current Profiler (ACDP) to sample the near-surface layers. Additionally, 30 RM11 external rotor Aanderaa currentmeters were distributed across the channel's vertical cross-section as shown in Figure 2. Table 1 describes the type of instruments used on each mooring and the depths at which measurements were obtained.

Tidal analysis of currents and transport

Ellipse parameters were determined for each of the frequencies, or tidal components, from harmonic analysis using the 'Matlab' t_tide program (Pawlowicz *et al*., 2002). This program is an adaptation of the FORTRAN routines by Foreman (1978). Sine waves of specific tidal frequencies are fitted by least squares. The length of the data series and the conventional Rayleigh criteria (taken as unity) allow up to 59 components or astronomically established frequencies for the tides, but this study was restricted to the two main

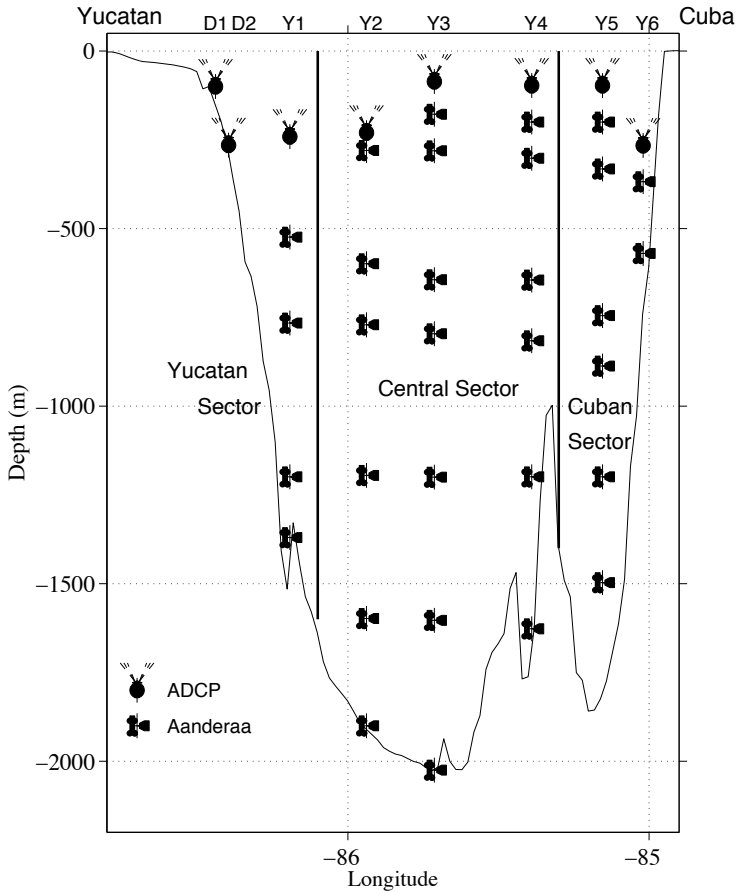

Fig. 2. Map of the Yucatan Channel's vertical section showing the distribution of currentmeters (ADCP.s and Aanderaa.s), and a division of the section in three sectors.

Table 1

Location and depth of the moored instruments, not all ADCPs bins were used

Mooring	Location		ADCPs		Depths of Aanderaas	Number of series
	W°	N°	Bin Thickness	Depths Covered		
D1	86.44	21.58	8	14 94		12
D2	86.40	21.58	10	30 250		23
Y1	86.18	21.53	8	29 261	560 803 1246 1409	34
Y2	85.91	21.59	8	28 268	291 644 817 1241 1644 1937	37
Y3	85.71	21.60	8	31 143	229 331 1251 1654 2067	22
Y4	85.47	21.73	8	24 128	234 336 680 852 1236 1659	20
Y5	85.27	21.86	8	25 130	793 935 1248 1531	18
Y6	85.02	21.80	8	28 252	380 583	31

diurnal tides K_1 and O_1, which are the major components, plus the two main semidiurnal constituents M_2 and S_2.

Maps of Tidal Ellipse Components

The ellipse tidal parameters are mapped in Figures 3 to 6. These parameters at 197 measuring points, each corresponding to a time series, are distributed irregularly and interpolated by Objective Mapping onto a uniform grid, thus building maps where contours are easy to visualize. The ellipse parameters are: 1) the major axis (M), 2) the minor axis (m), 3) the ellipse's inclination or geographic orientation (θ), and 4) the phase (ϕ), which specifies when the current maxima occur relative to that of the tidal potential in Greenwich (i.e. at longitude zero), and in general the vector velocity direction at any time. The eccentricity, defined by $\varepsilon = \sqrt{M^2 - m^2}\,/\,M$, measures how elongated the ellipse is, the sign of m, of the minor axis amplitude, is used to indicate if the vector velocity turns cyclonically (positive) or anticyclonically (negative). All the ellipse specifications are conventional (see, for example, The Open University, 1993). A statistical measure of interest, which is not an ellipse parameter, but specifies the confidence on a given parameter, is the signal to noise ratio, or for its initials, *snr*. In the maps shown, for simplicity, only the *snr* of M is reported.

Figures 3 and 4 show the O_1 and K_1 ellipse parameters, where similarities are of easy notice. The major axis is nearly uniform, close to 5 $cm{\cdot}s^{-1}$, from Yucatan to the center of the channel, with a near surface intensification towards the West and East, where it reaches 10 $cm{\cdot}s^{-1}$. The maxima, 16.5 and 19.5 $cm{\cdot}s^{-1}$ for O_1 and K_1, stand out at 1300 m depth on the eastern margin of the channel. The minor axis is smaller than 4 $cm{\cdot}s^{-1}$ throughout, and much smaller than the major axis, whence the eccentricity is close to one, expressing the elongation of the ellipses. The orientation (which is referred to the East, 90° being north) is mostly NNW aligned with the topography. The phase distribution does not define clear wave propagation, but shows a large gradient near the western shallow edge. In general the axes of K_1 are slightly larger than those of O_1.

The M_2 and S_2 ellipse components are shown in Figures 5 and 6. The M_2 and S_2 major axes, with averages close to 1 $cm{\cdot}s^{-1}$, and minor axes close to 0.1 $cm{\cdot}s^{-1}$, are much smaller than those of O_1 and K_1. Their orientations are, for the semidiurnal constituents, mostly NNW or N. The phase structure is nonetheless very complicated, and does not identify a propagation direction of the tidal wave. It does show a 6-hour lag from the earliest to the latest maximum arrival. The ellipse characteristics are quantitatively summarized in Table 2, separating averages over three vertical bands across the channel, as defined in Figure 2, and averaging the entire channel.

snr distributions.

The *snr* or signal-to-noise-ratio specifies how large the parameter of interest is relative to its error, or its uncertainty. If the *snr* equals one, the uncertainty is of the same magnitude as the estimate, if its *snr* is large, the estimate is well determined. For simplicity, in this study only the major axis *snr* is reported. An equivalent, or alternative, parameter

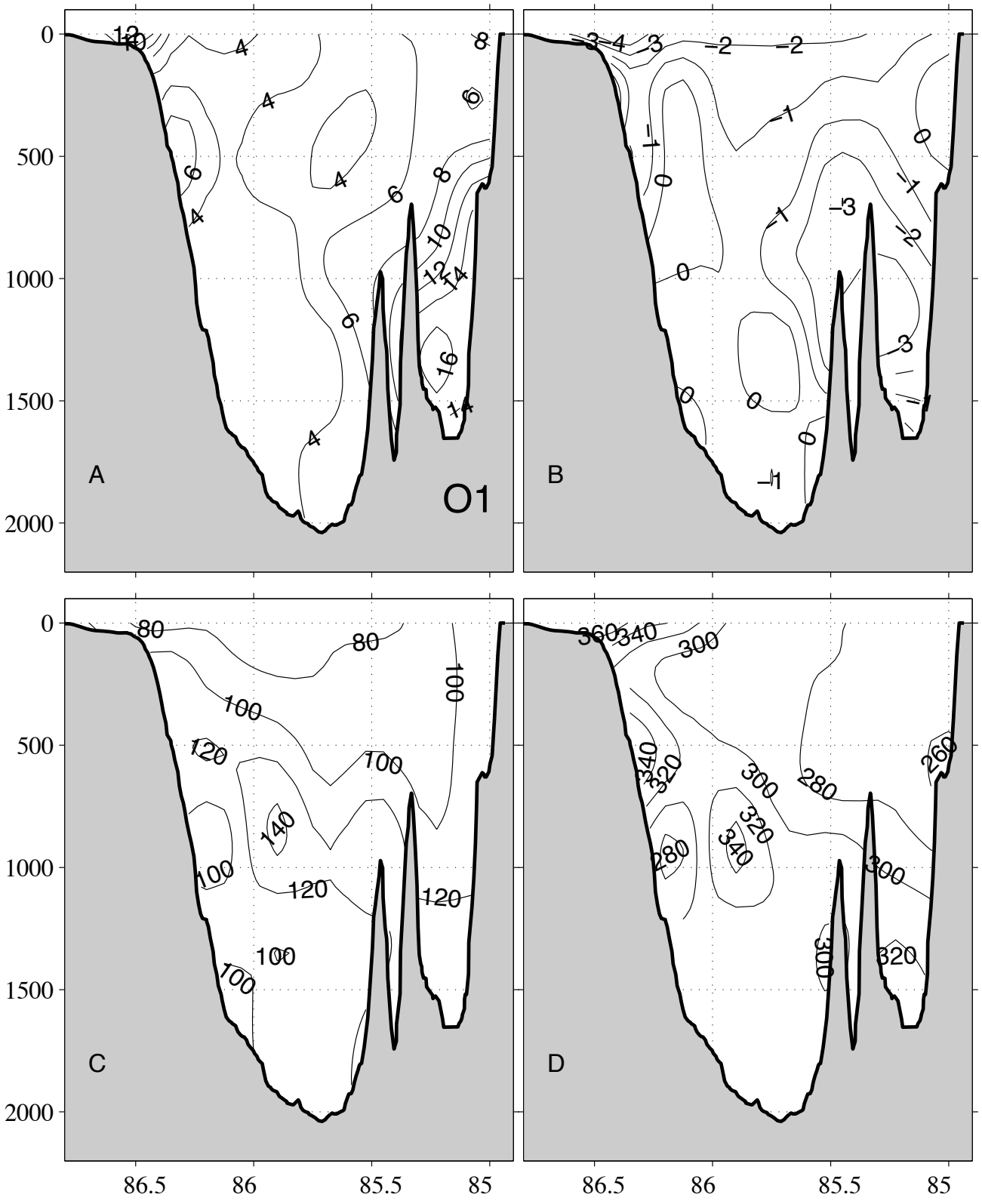

Fig. 3. Maps, abscissa is depth in *m*, ordinate is Longitude W°, of the ellipse components for the O_1 constituent: a) and b) amplitudes of major and minor axes in $cm{\cdot}s^{-1}$, c) orientation of major axis, in degrees relative to East, positive counterclockwise, and d) phase relative to tidal potential at Greenwich.

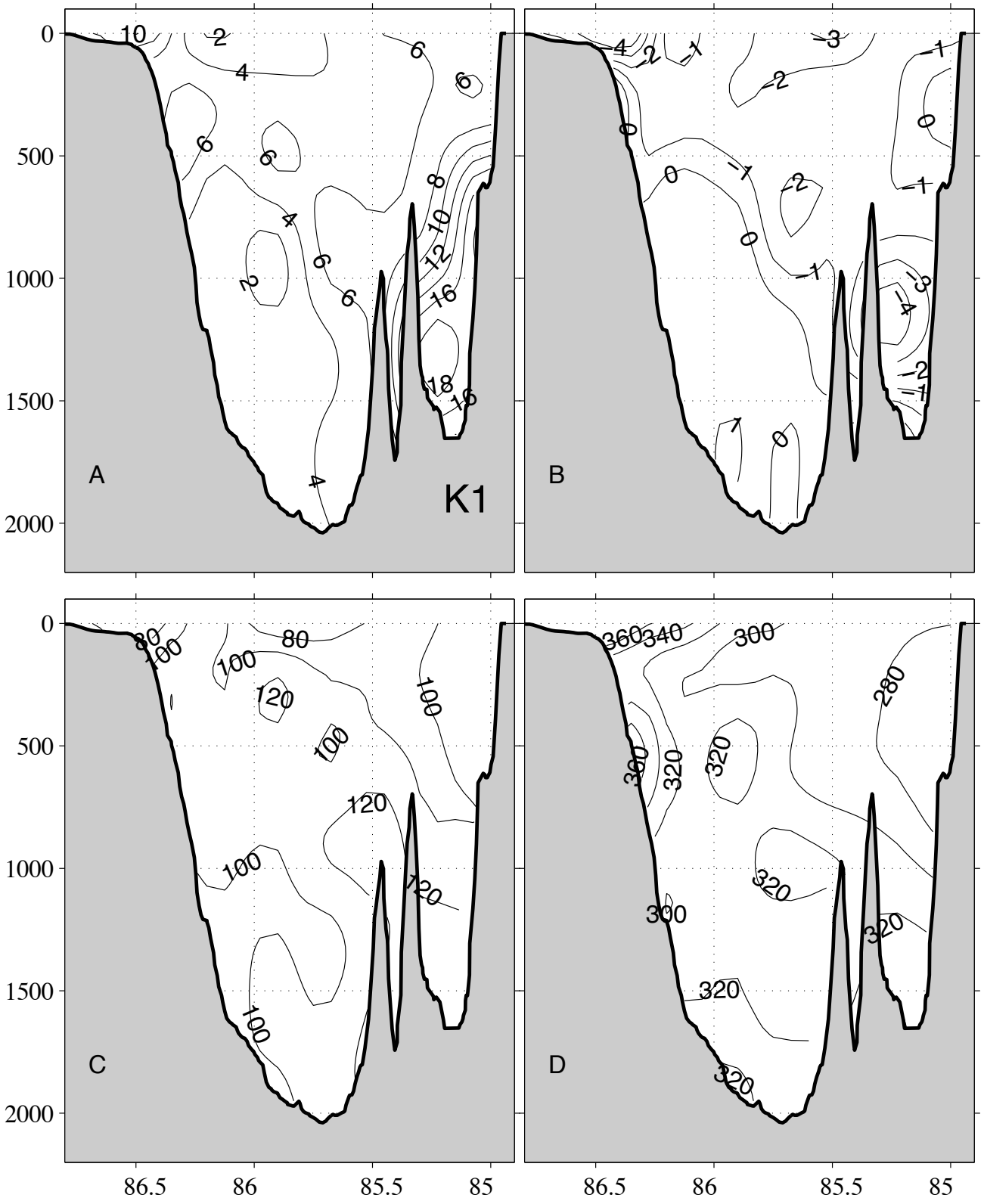

Fig. 4. Maps of the ellipse components for the K_1 constituent (same layout as in Figure 3).

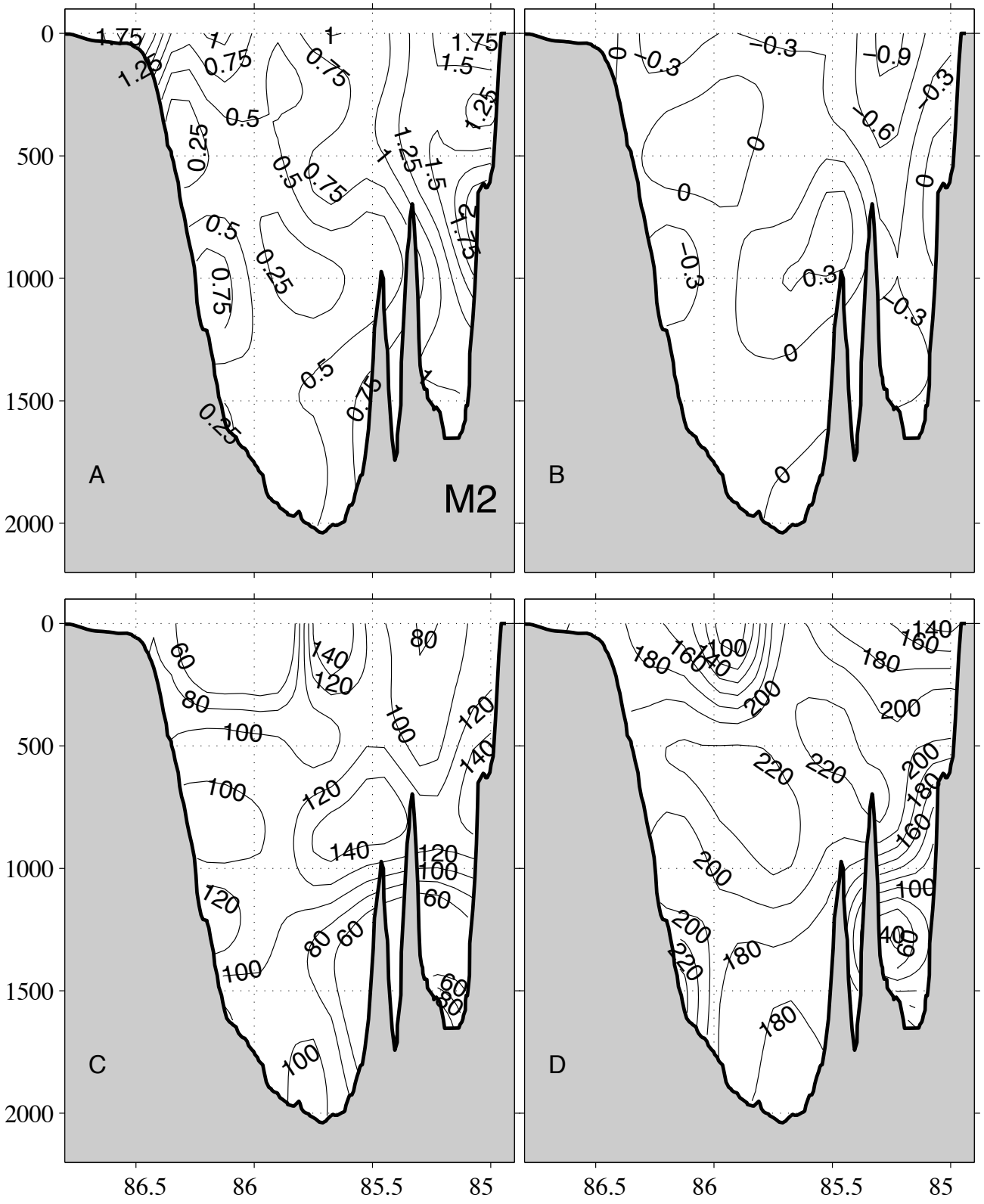

Fig. 5. Maps of the ellipse components for the M_2 constituent (same layout as in Figure 3).

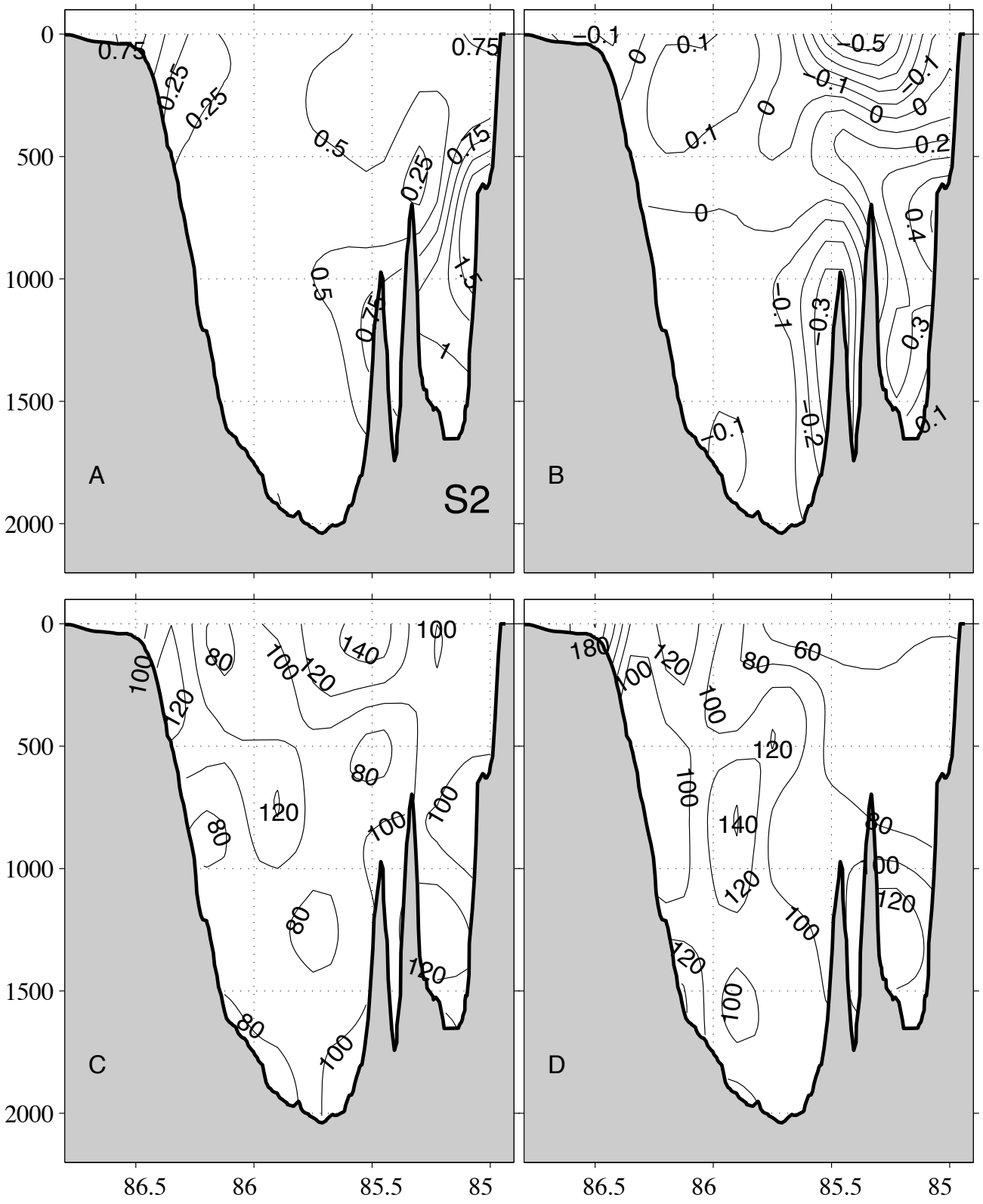

Fig. 6. Maps of the ellipse components for the S_2 constituent (same layout as in Figure 3).

Table 2

Average ellipse characteristics for the entire cross section of Yucatan Channel and each of the sections defined in Figure 2. The axes amplitudes are in $cm \cdot s^{-1}$, and ε, θ and ϕ are the eccentricity, orientation and phase

Constituent	Sector	Major Axis	Minor Axis	ε	θ	ϕ	*snr*
O_1	**Entire**	**6.63**	**-1.12**	**0.96**	**106**	**280**	**113**
	Yucatan	5.22	-1.43	0.94	98	256	29
	Central	4.69	-0.92	0.95	110	307	95
	Cuban	9.97	-1.02	0.98	112	282	215
K_1	**Entire**	**7.00**	**-1.05**	**0.95**	**104**	**283**	**133**
	Yucatan	5.31	-1.64	0.92	92	252	31
	Central	4.62	-0.43	0.94	110	311	91
	Cuban	11.06	-1.08	0.99	111	287	277
M_2	**Entire**	**0.99**	**-0.10**	**0.93**	**101**	**185**	**10**
	Yucatan	1.02	-0.06	0.90	98	199	3
	Central	0.60	-0.04	0.94	93	191	10
	Cuban	1.36	-0.21	0.95	112	165	16
S_2	**Entire**	**0.70**	**-0.10**	**0.93**	**101**	**107**	**5**
	Yucatan	0.68	-0.09	0.96	102	127	2
	Central	0.44	-0.10	0.93	95	114	6
	Cuban	0.92	-0.21	0.90	106	81	7

is the confidence interval; in the t_tide usage (Pawlowicz *et al*., 2002) the 95% confidence limits are given by δM with $snr = (M/\delta M)^2$. Thus $[(1-snr^{-1/2})\ M,\ (1+snr^{-1/2})M]$ is the 95% confidence interval for M.

Figure 7 shows maps of the *snr* distribution, one per constituent of interest. The distributions show for the two diurnal constituents large enough *snr*, averaging more than 120, indicating that these constituents are well-determined, especially in the deep and eastern margin, near Cuba. By contrast, the semidiurnal constituents show a distribution of *snr* with wide areas below 10, which manifests that the signal is poorly determined. Note that when the *snr* is larger than 100 the error is less than one tenth the estimated parameter and if the *snr* is below 9 the error is larger than one third the estimated parameter. The cause of low *snr* values is that in comparison with the continuum spectrum of the 'detided residual' integrated across a band of width 1/year contiguous to the tidal frequencies, the semidiurnal tides are weak and therefore highly contaminated by noise (Carrillo, 2001). If longer series were available, the same continuum spectrum of the residuals will not contaminate as much (*i.e*. the *snr* will be lower) because the band width disturbing the estimate will be thinner.

Tidal transport through the channel

The velocity component perpendicular to the vertical cross-section shown in Figure 2 allows, by straightforward integration, the calculation of the transport occurring between the Caribbean Sea and the Gulf of Mexico. Its time series has pronounced tidal signals with high *snr* for the constituents previously described (see Table 3). As explained before, from the length of the data and the conventional Rayleigh criteria, the harmonic analysis considers a set of 59 tidal constituents, of which only 12 are significant, with a *snr* larger than 2. These are, besides the ones in Tables 2 and 3, Q_1, RHO_1, NO_1, P_1, J_1, N_2, K_2 and M_4, which describe 91% (140 Sv^2) of the total transport variance (153 Sv^2). The most intense constituents are K_1, O_1, P_1, Q_1, M_2 and S_2 contributing with 45, 39, 4, 2, 0.4 and 0.3 percent wise and respectively in the total transport variance.

Conclusions

The diurnal O_1 and K_1 constituents are the dominant tidal currents in Yucatan Channel. The current ellipses for O_1, K_1, M_2 and S_2 have eccentricities close to one

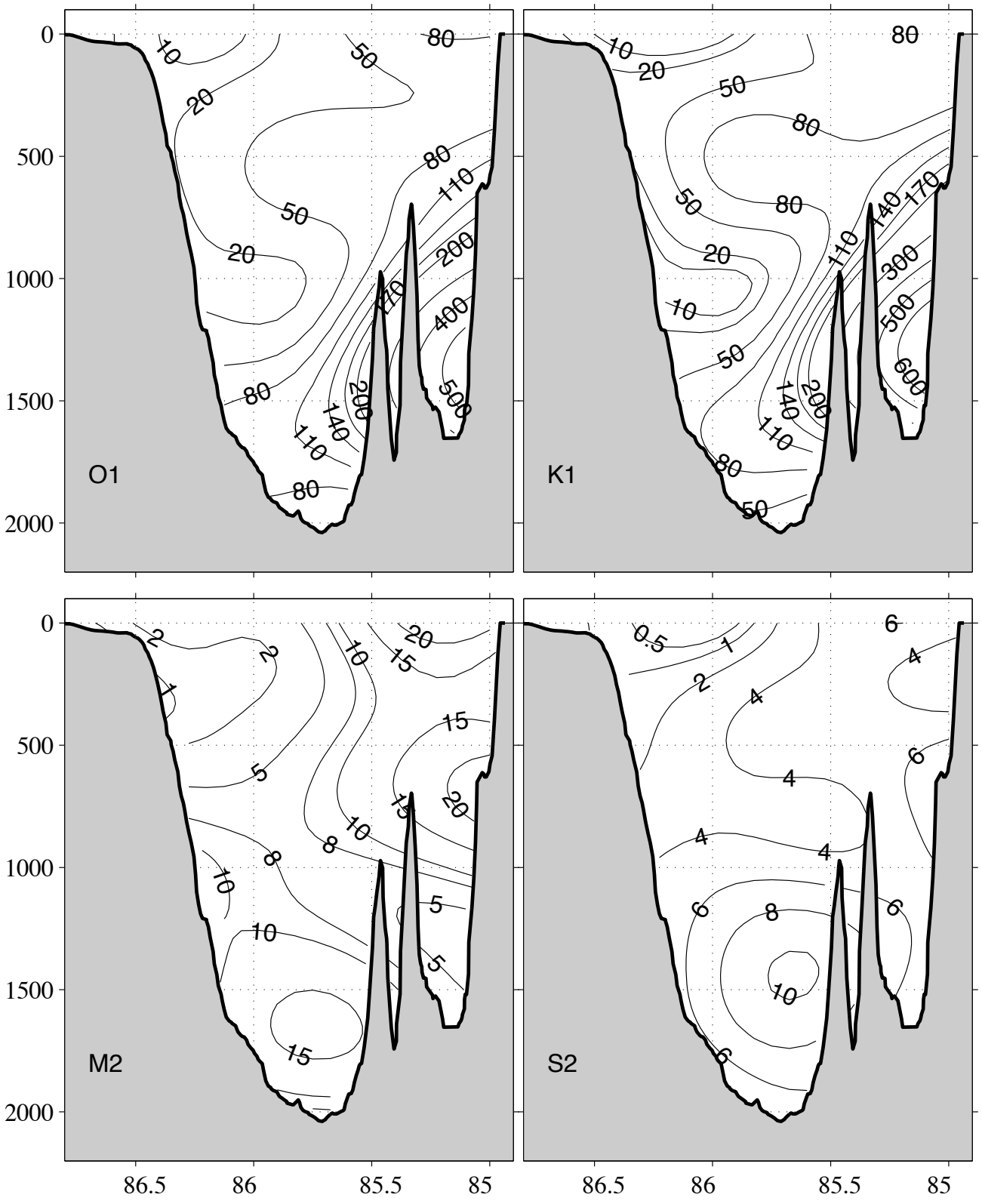

Fig. 7. Maps of the *snr* distribution (see text).

Table 3

Amplitude (in $10^6 m^3 \cdot s^{-1}$ or *Sv*) and phase (in degrees relative to the tidal potential at Greenwich) for the constituents contribution to the total transport. Confidence intervals are at 95%

Component	Amplitude	Phase	*snr*
O_1	11.7 ± 0.4	299 ± 2	1002
K_1	12.5 ± 0.4	308 ± 2	1201
M_2	1.2 ± 0.1	194 ± 7	63
S_2	1.0 ± 0.1	98 ± 8	50

and a preferential NNW orientation. The semidiurnal tidal signal is very weak, and poorly resolved. There is a deep, eastern region of the channel, on the Cuban margin, where tidal currents are intense and account for over 80% of the currents variance. The dynamical origin of such intensification remains unknown.

The transport through the Yucatan Channel has a variability dominated by tidal signals; approximately 91% of its variance is due to tides, mostly to the diurnal constituents. The O_1, K_1, M_2 and S_2 contributions in the transport signal through the Channel are 11.7, 12.5, 1.2 and 1.0 *Sv*. As for transport computation, velocities are integrated across the channel, noise is reduced and, consequently, even the comparatively weak semidiurnal contributions to transport are well-determined (see Table 3).

Acknowledgements

We thank the technical staff of the CANEK Project and the crew of the *B/O Justo Sierra* for their support. Funding was provided by Consejo Nacional de Ciencia y Tecnología (CONACyT), Centro de Investigación Científica y de Educación Superior de Ensenada (CICESE) and The DeepStar Consortium. Comments and corrections by Miguel Lavín and the anonymous reviewers were helpful.

Bibliography

BADAN, A., J. CANDELA, J. SHEINBAUM and J. OCHOA, 2005. Upper-layer circulation in the approaches to Yucatan Channel. *In:* Circulation in the Gulf of Mexico: Observations and Models. W. S. Sturges and A. Lugo-Fernandez, Eds. Geophysical Monograph Series 161. 57-69.

CARRILLO, F., 2001. Caracterización de las Corrientes de Marea en el Canal de Yucatán. M.S. Thesis, CICESE. pp. 86.

FOREMAN, M. G., 1978. Manual for tidal currents analysis and prediction. Institute of Ocean Sciences, Patricia Bay. Sidney, B.C. Pacific Marine Science Report 78-6.

HANSEN, D. V. and R. L. MOLINARI. 1979. Deep currents in the Yucatan Strait. *J. Geophys. Res., 84*, (C1), 359-362.

KJERFVE, B., 1981. Tides of the Caribbean Sea. *J. Geophys. Res., 86,* (C5), 4243-4247.

MAUL, G. A., D. A. MAYER, and S. R. BAIG. 1985. Comparisons between a continuous 3-year current meter observation at the sill of the Yucatan Strait, satellite measurements of Gulf Loop current area and regional sea level. *J. Geophys. Res., 90*, (C5). 9089-9096.

OCHOA, J., J. SHEINBAUM, A. BADAN, J. CANDELA and D. WILSON, 2001. Geostrophy via potential vorticity inversion in the Yucatan Channel. *J. Marine Res., 59,* 725-747.

PAWLOWICZ, R., B. BEARDSLEY and S. LENTZ, 2002. Classical tidal harmonic analysis including error estimates in MATLAB using T_TIDE, *Comput. Geosci., 28*, 929– 937.

SHEINBAUM, J., J. CANDELA, A. BADAN and J. OCHOA, 2002. Flow Structure and Transport in the Yucatan Channel. *Geophys. Res. Lett., 29*, (3), doi:10.1029/2001GL013990.

THE OPEN UNIVERSITY, 1993. Waves, Tides and shallow-water processes. Ed. By The Open University and Pergammon Press. New York. 187 p.

Fátima Carrillo González[1], José Ochoa[2,3,*], Julio Candela[2], Antonio Badan[2], Julio Sheinbaum[2] and Juan Ignacio González Navarro[2]

[1] Centro Universitario de la Costa, Universidad de Guadalajara, Guadalajara, Mexico
[2] Departamento de Oceanografía Física, Centro de Investigación Científica y de Educación Superior de Ensenada (CICESE), km. 107 Carretera Tijuana-Ensenada, Ensenada, Baja California, Mexico.
**Corresponding author: jochoa@cicese.mx*